JOURNAL OF GUIDANCE, CONTROL, AND DYNAMICS
Vol. 20, No. 2, March–April 1997

Design Impact of Piezoelectric Actuator Nonlinearities

John A. Main* and Ephrahim Garcia†
Vanderbilt University, Nashville, Tennessee 37235

Data are presented illustrating the need for inclusion of piezoelectric actuator nonlinearities if accurate system models are desired. The describing function approach was used in this investigation as an example. Whereas the use of the describing functions does improve overall accuracy of the system model, it is demonstrated that the extreme sensitivity of the describing functions to amplitude at low actuator displacements still compromises on the accuracy of system models that include voltage-controlled piezoelectric actuators. It is also demonstrated that using charge-feedback control with piezoelectric actuators makes the use of the nonlinear model elements less pressing since the charge control describing functions are much nearer unity than their voltage-control counterparts.

Nomenclature

A = actuator cross-sectional area, m^2
C = capacitance, F
c^D = stiffness at constant electric displacement, Pa
c^E = stiffness at constant electric field, Pa
D = electric displacement, C/m^2
d = piezoelectric constant, m/V
E = electric field, V/m
F = force, N
g = piezoelectric constant, m^2/C
K_{amp} = voltage-feedback amplifier gain, V/V
K_{as} = combined actuator, flexure, and amplifier gain, m/V
K_D = controller derivative gain, V/V
K_{OL} = open-loop system gain, m/V
K_p = controller proportional gain, V/V
K_{sg} = strain-gauge position feedback subsystem, V/m
k = spring constant, N/m
L = moment arm effective length, m
m = driven mass, kg
N = fundamental frequency representation of system nonlinearities
n = number of layers in stack actuator
Q = charge, C
R = resistance, Ω
S = strain
T = stress, Pa
t = piezoelectric material thickness, m
V_a = power amplifier input voltage, V
x = displacement, m

Introduction

In a previous paper,[1] describing functions were determined for piezoelectric actuators to quantify the amplitude dependence of their dynamic behavior. Describing functions were experimentally determined as a function of the amplitude of the stack displacement and frequency for a stack actuator using both voltage-feedback control and charge-feedback control approaches. The use of these describing functions in modeling piezoelectric actuator systems is further explored in this paper. Particular attention is paid to design issues such as predicting the performance of a system that includes piezoelectric actuators.

Received May 8, 1996; revision received Nov. 2, 1996; accepted for publication Nov. 11, 1996.

*Research Assistant Professor, Department of Mechanical Engineering; currently Assistant Professor, Department of Mechanical Engineering, 521 CRMS Building, University of Kentucky, Lexington, KY 40506. Member AIAA.

†Associate Professor, Department of Mechanical Engineering, Box 1592, Station B. Member AIAA.

This exploration is detailed in the following sections and proceeds as follows. First, a feedback position control system is designed, and stability limits are predicted using describing functions to account for the nonlinear behavior of the piezoelectric actuators. These describing functions were determined in a previous paper for an identical piezoelectric stack actuator. Next, the stability limits of the prototype system are found experimentally using both voltage-feedback and charge-feedback control strategies in separate tests. Finally, conclusions are drawn about how the results of this work should impact the piezoelectric actuator system design process by examining 1) the characteristics of the describing functions themselves and 2) comparing the system performance predictions to the experimental results obtained.

Prototype Position Control System

A typical task for a miniature actuator is fine position control, and so in this study a position feedback system was designed around a piezoelectric actuator. A sketch of the complete position control system is shown in Fig. 1. The system consists of four major components: the actuator assembly, the power amplifier (which can be voltage feedback or charge feedback, see Ref. 2 for a comparison), the proportional-derivative (PD) controller, and a strain gauge for position feedback. The actuator assembly, shown in detail in Fig. 2, is a piezoelectric stack mounted in a mechanism that is used to amplify the displacement output of the stack with a four-bar flexure linkage. This mechanism has two cascaded moment arms attached to a base by flexure hinges to amplify the motion of the piezoelectric stack. This assembly was designed to be one of three actuators for a mirror in an adaptive optics application. A small mass was mounted at the output point of the actuator to substitute for the mirror inertia.

A top-level block diagram of the control system is shown in Fig. 3. In this diagram the system is broken up into four major blocks, which are detailed subsequently: the PD controller, the strain gauge position feedback element (K_{sg}), the actuator/flexure/amplifier subsystem K_{as}, and an inverter that is used in conjunction with the charge-feedback amplifier. Each of these components now is discussed in detail.

PD Controller

The proportional component of the controller is a simple inverting amplifier with transfer function and gain range of

$$K_P(s) = -R_f/10^4; \quad R_f = 0 \rightarrow 10^4 \tag{1}$$

R_f is the value of the feedback resistor in ohms.

The controller derivative component combines a differentiator and a low-pass filter. The resulting transfer function is

$$K_D(s) = \frac{-0.1e^{-6}R_2}{(0.1e^{-9}R_2 s + 1)(0.2e^{-3}s + 1)}; \quad R_2 = 0 \rightarrow 300 \tag{2}$$

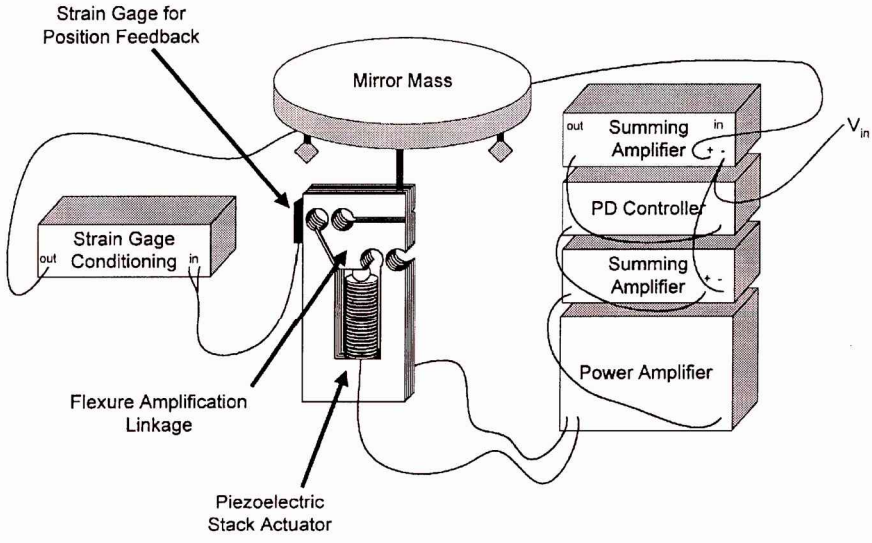

Fig. 1 Schematic of the breadboard piezoelectric actuator position control system.

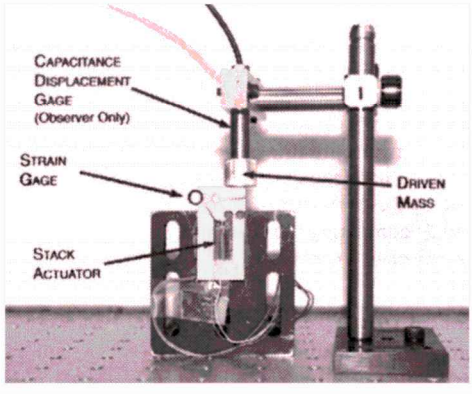

Fig. 2 Photograph of piezoelectric stack actuator and flexure amplification stage.

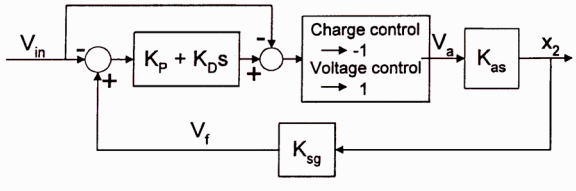

Fig. 3 Block diagram of the feedback control system.

Position Feedback

A strain gauge mounted on a flexure hinge (location shown in Fig. 2) provides displacement feedback to generate the error signal used by the PD controller. Using this element as position feedback assumes that the output arm of the flexure linkage is absent of dynamic effects, which was experimentally verified by comparing the strain gauge output to the output of the independent observer (see Fig. 2) during dynamic testing. The position feedback path also contains a low-pass filter, resulting in a transfer function of

$$K_{sg}(s) = \frac{0.4e^6}{6.62e^{-6}s + 1} \tag{3}$$

Actuator/Flexure/Amplifier Subsystem

The block labeled K_{as} is defined as the flexure output displacement x_2 relative to a voltage input to the actuator power amplifier

$$K_{as} = x_2 / V_a \tag{4}$$

where V_a is the input signal to the power amplifier. The dynamics of three elements are included in K_{as}: the piezoelectric stack, the flexure amplification stage, and the amplifier that drives the stack. Because voltage-feedback control and charge-feedback control rely on different piezoelectric constitutive equations for control relationships, and both are of interest to this study, K_{as} will have a distinct form in each case.

Voltage Control

This position control system utilizes piezoelectric stack actuators to provide the motive force. Piezoelectric stack actuators are generally constructed so that stresses, strains, and electric fields are limited to the 3 direction of the material. By simplifying the constitutive relationships for piezoelectric materials, one possible Hooke's law for the piezoelectric material is

$$T_3 = c_{33}^E S_3 - d_{33} c_{33}^E E_3 \tag{5}$$

where T_3 is the stress in the 3 direction, S_3 the strain, E_3 the total electric field, c_{33}^E the modulus of the material at constant electric field, and d_{33} a piezoelectric constant.[3]

This constitutive equation can be used to develop a control relationship by relating the state variables to appropriate input and output quantities. The strain in the material (S_3) is related to the overall displacement of the stack by

$$S_3 = x_1 / nt \tag{6}$$

where x_1 is the stack tip displacement, n the number of layers of piezoelectric material in the stack, and t the thickness of the layers.

The electric field E_3 in the piezoelectric material and the amplifier output voltage are related by

$$E_3 = \frac{K_{\text{amp}} V_a}{t} \tag{7}$$

In this investigation $K_{\text{amp}} = -10$, and the bandwidth of interest was limited to the linear region of the amplifier.

The piezoelectric stack is mounted in an aluminum flexure mechanism that is used to amplify the output displacement. Assuming a compressive force F on the piezoelectric stack, the stress is

$$T_3 = -F/A \tag{8}$$

where A is the cross-sectional area of the stack; substitution of Eqs. (6–8) into Eq. (5) yields a control relationship for the stack actuator coupled to the voltage feedback amplifier:

$$F = -\frac{c_{33}^E A x_1}{nt} + \frac{d_{33} c_{33}^E A K_{\text{amp}} V_a}{t} \tag{9}$$

F and x_1 represent the force and the displacement at the input point of the flexure stage, and so the next logical step is to relate these quantities to their analogs at the flexure output point.

The flexure stage serves to amplify the displacement output of the piezoelectric stack by using levers and hinges machined from a solid block of aluminum. The flexure is not a perfect mechanical amplifier, however, because there is stiffness in the flexure hinges. If

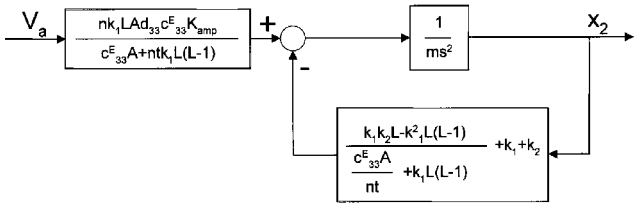

Voltage feedback control

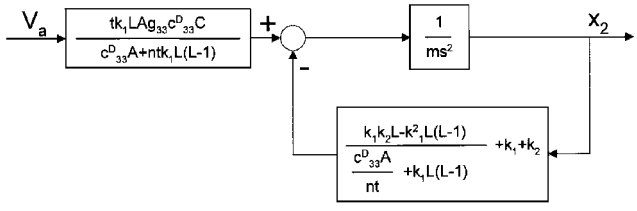

Charge feedback control

Fig. 4 Block diagram models of K_{as}.

the flexure stiffness between the actuator input and output points is taken to be k_1 and the stiffness between the output point and ground is k_2, the dynamic equations for the flexure stage can be written by summing the forces on the driven mass. This results in

$$m\ddot{x}_2 = k_1(Lx_1 - x_2) - k_2x_2 \tag{10}$$

where L is the flexure amplification, x_1 is the displacement of the input point of the flexure stage, and x_2 is the displacement of the output point. Summing the forces acting on ground results in

$$0 = k_1(L-1)(Lx_1 - x_2) - F + k_2x_2 \tag{11}$$

Values for the spring constants k_1 and k_2 were determined by using Eqs. (10) and (11) and the finite element model of the flexure stage. The deflection range of interest was small and all loads were in the elastic region and so the resulting force-displacement relationship was assumed to be linear. This allowed one set of force-displacement values derived from the finite element model to be substituted into Eqs. (10) and (11) and solved simultaneously for k_1 and k_2. The values determined were $k_1 = 60.9$ kN/m and $k_2 = 43.9$ kN/m.

The dynamic equation for the voltage control embodiment of K_{as} is found by combining Eqs. (9–11) and eliminating variables F and x_1. The resulting relationship is shown as a block diagram in Fig. 4.

Charge Control

A similar line of reasoning is used to develop an alternate control relationship for the piezoelectric stack actuator driven by a charge-feedback power amplifier. The following constitutive relationship assumes all state variables are again limited to the 3 direction:

$$T_3 = c_{33}^D S_3 - g_{33}c_{33}^D D_3 \tag{12}$$

where c_{33}^D is the modulus of the piezoelectric material at constant electric displacement, g_{33} is a piezoelectric constant, and D_3 is the electric displacement in the 3 direction. The electric displacement control relationship relies fundamentally on the amount of free charge in the system. Gauss' law is used to relate the electric displacement to the free charge and results in

$$D_3 = Q/nA \tag{13}$$

where Q is the total amount of free charge applied to the n layers of the stack.

Substituting in this result as well as Eqs. (6–8) yields a piezoelectric stack actuator control relationship that relies fundamentally on applied charge:

$$F = \frac{-c_{33}^D Ax_1}{nt} + \frac{g_{33}c_{33}^D Q}{n} \tag{14}$$

A number of methods for controlling the amount of charge on a piezoelectric actuator have been put forth in the literature. One places a capacitor in series with the piezoelectric load so that the total capacitance is dominated by the reference capacitance and, therefore, the charge in the system is explicitly known.[4,5] Activating a current source for precise periods has also been demonstrated as a method for delivery of precise amounts of charge to piezoelectric actuators.[6] The strategy used in this work for controlling the amount of charge applied to a piezoelectric stack was presented by Comstock.[7] The Comstock circuit relates the charge present on a piezoelectric actuator Q to an input voltage V_a through

$$Q = CV_a \tag{15}$$

where C is the value of a capacitor in the circuit. Note that this is a noninverting amplifier. This necessitates the additional inverter in the control system to ensure stability when using charge control (see Fig. 3). Substituting this result into Eq. (14) yields a charge-feedback control relationship for the piezoelectric stack coupled to the charge-feedback amplifier:

$$F = \frac{-c_{33}^D Ax_1}{nt} + \frac{g_{33}c_{33}^D CV_a}{n} \tag{16}$$

This relationship is then combined with Eqs. (10) and (11) to determine the charge control version of K_{as}. The resulting relationship is also shown as a block diagram in Fig. 4.

Both the charge-feedback and voltage-feedback K_{as} models were experimentally verified by obtaining open-loop transfer functions of the displacement of the driven mass relative to voltage input into the respective amplifiers. The results of this experimental verification are presented in Figs. 5 and 6 for voltage control and charge control,

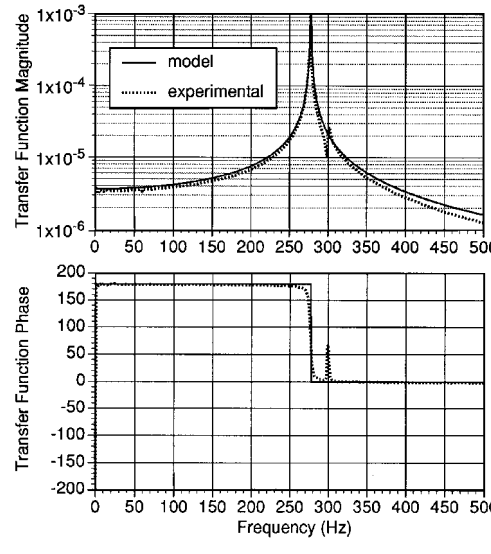

Fig. 5 Experimental and theoretical K_{as} using voltage-feedback control.

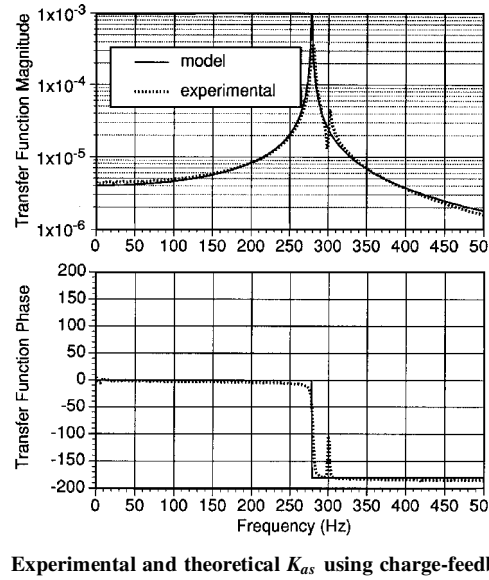

Fig. 6 Experimental and theoretical K_{as} using charge-feedback control.

Table 1 Actuator, material, and structural parameters

Stack parameters	
Number of layers n	130
Layer thickness t	1.20×10^{-4} m
Stack cross-sectional area A	3.46×10^{-5} m^2
Material constants	
Piezoelectric constant d_{33}	568×10^{-12} m/V
Constant field modulus c_{33}^E	67.5 GPa
Piezoelectric constant g_{33}	23.3×10^{-3} V-m/N
Constant electric displacement modulus c_{33}^D	111 GPa
Flexure stage parameters	
Ideal flexure amplification L	8.6
Spring constant k_1	60.9 kN/m
Spring constant k_2	43.9 kN/m
Driven mass m	34 g
Amplifier parameters	
Voltage amplifier gain K_{amp}	-10
Charge amplifier series capacitance C	10 μF

respectively. The tests were performed at very small displacements and are bandwidth limited (dc 500 Hz) to avoid any amplitude-dependent effects. The variable values used to generate the model curves are listed in Table 1.

Predicting Maximum System Gains

A method for prediction of phase and stability margins (and therefore maximum system gains) for systems including piezoelectric actuators was presented previously and is based on the describing function method of stability analysis.[1] A brief synopsis is included here.

Using the open-loop gain of a feedback control system to evaluate system stability margins requires finding solutions for the equation

$$-1 = K_{OL}(s) \tag{17}$$

The describing function method takes a known system nonlinearity and approximates it with a linear fundamental frequency representation, conventionally labeled N. Stability margins and maximum gains are calculated from solutions to the equation

$$-1/N = K_{OL}(s) \tag{18}$$

where N represents the system nonlinearities and K_{OL} represents the linear portion of the system open-loop gain. The function or group of functions represented by N are generally referred to as describing functions. The functions $-1/N$ then play the role that the $-1 + 0i$ point plays in Nyquist stability analysis.

The system nonlinearities must be known for the piezoelectric actuator feedback control system to solve Eq. (18). All of the control system elements in the prototype system under investigation here are known to behave linearly over the range of test conditions with the exception of the piezoelectric stacks, which can display nonlinear effects such as hysteresis and amplitude dependence. Unfortunately the nonlinearities involved in piezoelectric stack control are not known a priori. In an earlier study, this problem was addressed by applying a known sinusoidal signal (be it voltage or charge) to a piezoelectric stack in an easily modeled simple system and recording the displacement response.[1] The piezoelectric stack nonlinearities were then determined a posteriori by reducing the differences between the dynamic behavior of the physical system and the linear system model to a fundamental frequency representation. This operation was repeated over a range of frequencies and input signal amplitudes to map the actuator describing function. A stack identical to the one from the previous study was used here, and so it is assumed that the nonlinearities will also be identical.

That the stack nonlinearities are the same in two identical stack actuators is one of the two main assumptions in this method. The second is that the calculated nonlinearities from one system can be used by analogy to predict the stability of another system that may have different load-displacement characteristics, but uses the same piezoelectric stack actuator.

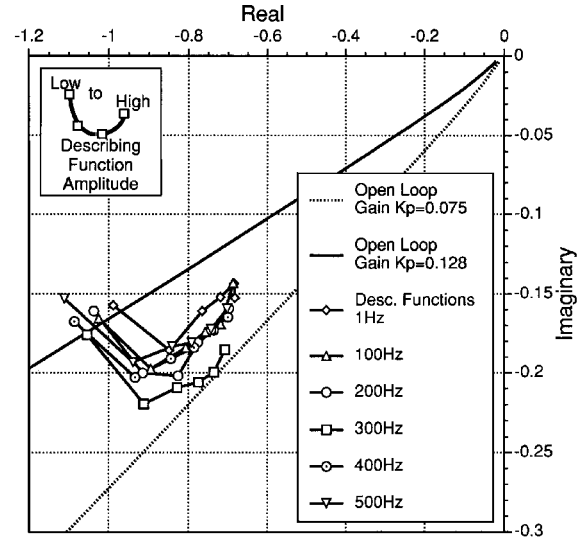

Fig. 7 Determination of the amplitude dependent maximum system K_p using voltage feedback.

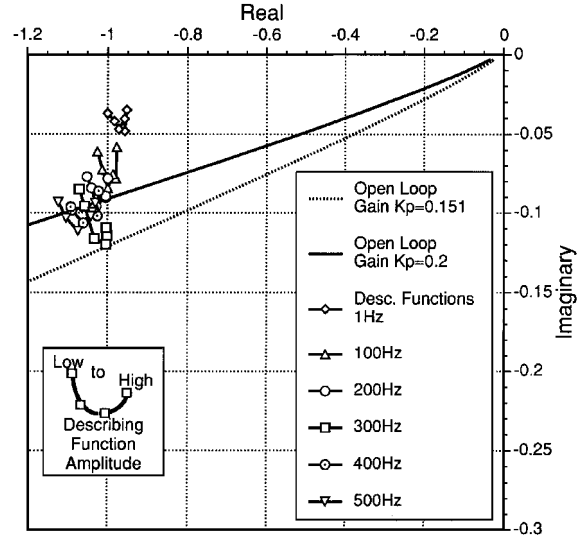

Fig. 8 Determination of the amplitude dependent maximum system K_p using charge feedback.

The $-1/N$ functions for the stack actuator used in this study are plotted in the complex plane in Figs. 7 and 8 for voltage-feedback and charge-feedback control, respectively. There are six describing function curves in each plot, covering a dc 500-Hz range in 100-Hz increments. Each symbol corresponds to a particular frequency, and the lines connecting like symbols show the amplitude dependence of the describing function at that frequency. The describing functions were determined for stack deflections of 1–6 μm in 1-μm increments. The maximum voltage applied to the stack was 54 V, and all describing functions were determined with the simple stack-mass system operating well below resonant frequency to avoid dynamic effects.

The position of the describing functions relative to the open-loop gain curve of the feedback control system illustrates the relative stability of the system. For example, the two open-loop gain curves in Fig. 7 were calculated for the prototype position control system using the voltage-feedback model. Each curve represents a critical value for the proportional gain K_p. The lower curve represents a proportional gain (K_p) equal to 0.075 V/V, and the upper curve is the result of increasing that gain to 0.128 V/V. The open-loop gains were calculated from the system model with the differential gain resistor value (R_2) set at 147.5 Ω.

The lower curve was calculated using the maximum proportional gain that can be applied before the open-loop gain curve

intersects any of the describing functions. Because it considers all of the voltage-feedback describing functions as critical points, it is a prediction of the maximum proportional gain possible in the system using voltage-feedback control. The upper curve represents the maximum open-loop gain that can be achieved before the open-loop gain curve intersects any of the lowest amplitude points of the voltage-feedback control describing functions. Because it considers only the lowest amplitude points of the voltage-feedback describing function to be critical points, it is a prediction of the maximum K_p possible if the system is operated only at low amplitudes.

The open-loop gain curves in Fig. 8 were calculated using the charge-feedback K_{as} model with a the differential gain resistor set to 125 Ω to account for the difference in internal damping in the two amplifier embodiments. The differential gain was adjusted to yield equivalent ζ values for the overall system to make the two systems as equivalent as possible. The K_p values for the lower and upper curves are 0.151 and 0.200, respectively (see Table 2). The lower and upper curves represent the maximum high and low amplitude K_p possible under charge-feedback control.

Experiment

An experimental determination of the maximum proportional gains this system can tolerate when driven over a range of amplitudes was performed. This was accomplished by adjusting the amplitude of an input noise signal while K_p was set to zero until a desired target mass amplitude was achieved. The proportional gain K_p was subsequently increased until the system exhibited instabilities. The instabilities noted in these maximum gain tests typically appeared as high-frequency system oscillations in the charge-feedback system and severely degraded transfer functions in the voltage feedback system, indicating that differences in the two control embodiments still exist despite efforts to make the systems as identical as possible. The test was repeated four additional times at the same input noise level to determine an average critical K_p at that amplitude. Five output amplitude levels were considered using both voltage-feedback and charge-feedback control. In the first test in each series, the mass displacement amplitude was set to 2 μm overall rms (0–500 Hz frequency range) with K_p set to zero. Subsequent tests increased the output amplitude in 2-μm rms increments until a maximum of 10-μm rms was reached. At approximately the 10-μm rms output amplitude the maximum stack voltage corresponded to the voltage used to determine the high-amplitude describing functions.

The results of the maximum K_p tests are shown in Figs. 9 and 10 as well as Tables 3 and 4. The maximum gains shown are not directly comparable between voltage-feedback and charge-feedback control because the two amplifier configurations use different forms of the piezoelectric constitutive relationships and, therefore, have distinct inherent gains, as reflected by the two variations of K_{as}.

Table 2 Predicted critical K_p values

Critical values of K_p for voltage control	Critical values of K_p for charge control	Open-loop gain plot
0.075	——	Fig. 7
0.128	——	Fig. 7
——	0.151	Fig. 8
——	0.200	Fig. 8

Table 3 Experimentally determined maximum K_p values under voltage-feedback control as a function of input signal amplitude

Input white noise level, mV rms	Displacement output at $K_p = 0$, μm overall rms	Maximum K_p
60	1.986	0.1646
120	4.090	0.1570
180	6.082	0.1281
240	8.291	0.1035
290	10.05	0.0768

Table 4 Experimentally determined maximum K_p values under charge-feedback control as a function of input signal amplitude

Input white noise level, mV rms	Displacement output at $K_p = 0$, μm overall rms	Maximum K_p
50	2.045	0.1970
100	3.962	0.1899
160	6.165	0.1763
205	7.885	0.1782
260	10.05	0.1621

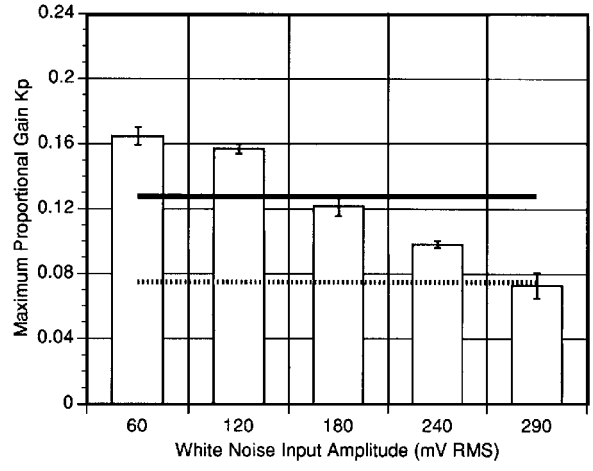

Fig. 9 Theoretical/experimental maximum K_p for voltage-feedback control as a function of output amplitude: □, experimental determined maximum K_p (SSD); ▬, predicted maximum gain at low amplitudes; and ıııı, predicted maximum gain at high amplitudes.

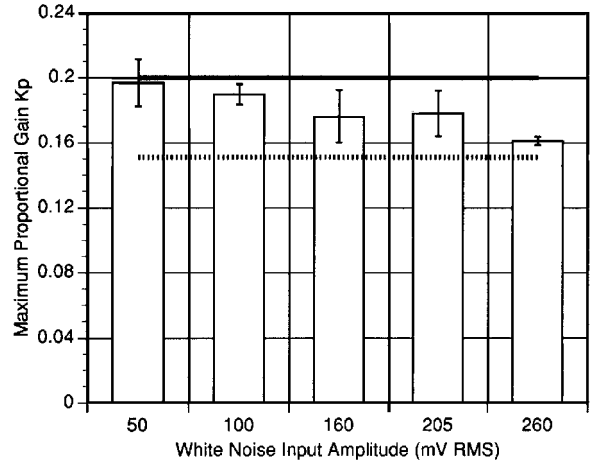

Fig. 10 Theoretical/experimental maximum K_p for charge-feedback control as a function of output amplitude: □, experimental determined maximum K_p (SSD); ▬, predicted maximum gain at low amplitudes; and ıııı, predicted maximum gain at high amplitudes.

Discussion

The goal is to examine design issues associated with systems that utilize piezoelectric actuators for positioning tasks. The design issue under particular scrutiny is the accuracy of piezoelectric system models, regardless of whether voltage feedback or charge feedback is the control strategy of choice. One of the engineers goals is to accurately predict the behavior of a dynamic system so that design trades can be accomplished before resources are invested in static hardware. This places a premium on the accuracy of system models because inaccurate models will directly impact the quality of engineering trades.

The describing function method is useful for representing system nonlinearities, and examination of the $-1/N$ curves in Figs. 7 and 8 demonstrate their value in modeling piezoelectric actuator systems. Piezoelectric actuators under both voltage-feedback and

charge-feedback control exhibited significant nonlinear behavior, as indicated by the spread of the $-1/N$ loci. This spread represents a reduction in stability limits of systems that include piezoelectric actuators because the system will exhibit instabilities well before the open-loop gain curve intersects the $-1 + 0i$ point on the complex plane. This is especially true in the case of voltage control. While the charge-feedback control points remain in the immediate vicinity of $-1+0i$, the voltage control $-1/N$ functions exhibit extreme amplitude dependence, even varying in magnitude up to 40%. This has a direct impact on the system design process. The existence of uncertain component behavior in a dynamic system forces extremely conservative design choices for the system as a whole. Perhaps the lesson to be learned from examination of the stack actuator describing functions is that the nonlinear characteristics of piezoelectric actuators, particularly under voltage control, must be accounted for somehow if accurate system models are to be generated. The same could also be said for charge-feedback control, but the nonlinear effects are less extreme.

The describing functions determined for the voltage-feedback and charge-feedback systems quantify the system nonlinearities. Nonlinear system behavior can be reasonably assumed to arise from either the mechanical system (the flexure), the power electronics, or the electromechanical interface. The flexure mechanism was limited to small deflections and elastic stresses, and so it is reasonable to assume that it is not the source of these nonlinear effects. The voltage-feedback and charge feedback amplifiers were tested off-line for linearity by monitoring their output voltage while driving a purely capacitive load. Both demonstrated only linear behavior. The only remaining source for the differences between voltage control and charge control is the electromechanical interface, as represented by the constitutive equations [Eqs. (5) and (12)]. This series of tests on piezoelectric actuator systems indicates that the discrepancies between models and the real piezoelectric system performance arise from modeling the piezoelectric effect as purely a linear phenomenon.

The necessity of using describing functions to model system behavior accurately is evident from Figs. 7 and 8, but this raises the question of how accurate this method is for modeling piezoelectric systems. The experiment described in the preceding sections was performed specifically for this evaluation. The maximum K_p values listed in Tables 3 and 4 are plotted as a function of output deflection in Figs. 9 and 10 for voltage-feedback and charge-feedback control, respectively. Each datum point represents the average experimental maximum K_p and the error brackets the 90% confidence interval on the experimental results. Also shown on each plot are two horizontal lines. The upper line is the maximum low-amplitude K_p predicted by the system model with describing functions, and the lower line the maximum K_p predicted for high amplitudes, also using the describing functions. It is striking that the maximum gains were accurately predicted in both of the high-amplitude cases, yet in only the low-amplitude charge control case. There is a large discrepancy between the predicted and experimental maximum K_p value for low-amplitude voltage control.

This error can be explained by looking at the sensitivity of the describing functions as a function of stack output amplitude. The average sensitivity of the describing functions as a function of amplitude are shown in Fig. 11. These plots were generated by calculating the sensitivities of the magnitude and phase portions of the actuator describing functions at each frequency, then averaging those results into one composite describing function sensitivity each for voltage-feedback control and charge-feedback control. Examination of Fig. 8 indicates that a large error in predicting the low-amplitude K_p in voltage control is completely understandable. This region displays the greatest sensitivity to stack output amplitude in both the magnitude and phase plots. This is especially interesting because this is the region where the most linear behavior of voltage controlled piezoelectric actuators is claimed to be found. Although hysteresis and amplitude dependence may be small here, this is the region in which both of these quantities are changing most rapidly, and this alone will inject uncertainty into the system design process. This is true whether or not the piezoelectric actuator nonlinearities are accounted for in the system model.

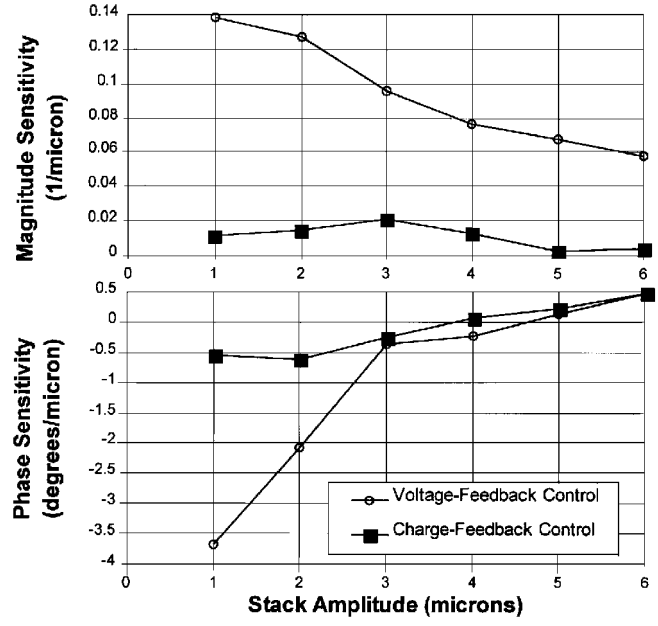

Fig. 11 Piezoelectric actuator describing function sensitivity as a function of stack displacement amplitude.

Conclusions

The system design process requires accurate component models, and piezoelectric actuators are not well suited to accurate linear modeling. It is demonstrated that accurate modeling of systems that include piezoelectric actuators requires incorporation of the actuator nonlinearities in some fashion. Here this was accomplished with a describing function approach. It is further shown that problems can arise even in the case where the actuator nonlinearities are included in the model. Significant modeling errors arose in this investigation because of the high sensitivity of voltage control describing functions to amplitude at lower amplitudes.

The describing functions presented were determined for a specific piezoelectric actuator under both voltage control and charge control. It is not unreasonable to assume that similar actuators made of layers of PZT-5H will have similar characteristics. However, generalization of these specific describing functions to significantly different actuator designs is not directly supported by this work. One important characteristic that does appear to be a general characteristic of piezoelectric actuators is that the system nonlinearities under both voltage control and charge control act to progressively reduce system stability with increasing amplitude.

References

[1]Main, J., and Garcia, E., "Errors and Accuracy in Modeling Piezoelectric Stack Actuators," *Proceedings of the Tenth VPI&SU Symposium on Structural Dynamics and Control* (Blacksburg, VA), 1995, pp. 65–76.

[2]Main, J., Garcia, E., and Newton, D., "Precision Position Control of Piezoelectric Stack Actuators," *Journal of Guidance, Control, and Dynamics*, Vol. 18, No. 5, 1995, pp. 1068–1073.

[3]Anon., "IEEE Standard on Piezoelectricity," American National Standards Inst./Inst. of Electrical and Electronics Engineers, ANSI/IEEE Std. 176-1987, Inst. of Electrical and Electronics Engineers, New York, 1988.

[4]Kaizuka, H., and Siu, B., "A Simple Way to Reduce Hysteresis and Creep When Using Piezoelectric Actuators," *Japanese Journal of Applied Physics*, Vol. 27, No. 5, 1988, pp. L773–L776.

[5]Anderson, E., Moore, D., Fanson, J., and Ealey, M., "Development of an Active Member Using Piezoelectric and Electrostrictive Actuation for Control of Precision Structures," *Proceedings of the AIAA/ASME/ASCE/AHS/ASC 31st Structures, Structural Dynamics, and Materials Conference* (Long Beach, CA), AIAA, Washington, DC, 1990, pp. 2221–2233 (AIAA Paper 90-1085).

[6]Newcomb, C., and Flynn, I., "Improving the Linearity of Piezoelectric Ceramic Actuators," *Electronics Letters*, Vol. 18, No. 11, 1982, pp. 442, 443.

[7]Comstock, R. H., "Charge Control of Piezoelectric Actuators to Reduce Hysteresis Effects," U.S. Patent 4,263,527, April 1981.